IOSR Journal Of Pharmacy And Biological Sciences (IOSR-JPBS)
e-ISSN:2278-3008, p-ISSN:2319-7676. Volume 16, Issue 4 Ser. III (Jul. – Aug. 2021), PP 37-46
www.Iosrjournals.Org

Molecular studies on the therapeutic effects of Mn-Zn-Fe_2O_4/Se nanocomposite for hyperthermia treatment on liver cancer

Huda Y. Gedawy[1,2], Hemely A. Hassan[1], A. A. Ebnalwaled[2,3*], Nadia S. Mahrous[1]

[1]*Zoology Department, Faculty of Science, South Valley University, 83523, Qena, Egypt.*
[2]*Electronics and Nano Devices Lab, Physics Department, Faculty of Science, South Valley University,Qena, 83523 Egypt*
[3]*Faculty of Nanotechnology for Postgraduate Studies, Cairo University, Sheikh Zayed Campus, 6th October City, Giza, 12588, Egypt*

Abstract
In this paper, we studied the effect of Mn-Zn-Fe_2O_4/Se nanocomposite which was synthesized by coprecipitation method and investigated its therapeutic effect that induced by an alternating magnetic field on xenograft liver cancer in mice. Mn-Zn-Fe_2O_4/Se was described by X - ray diffraction (XRD), transmission electron microscopy (TEM) and Fourier transform infrared spectroscopy (FTIR).We also studied cytotoxicityof Mn-Zn-Fe_2O_4/Se nanocomposite on the HepG2 cell line. The cytotoxicity results revealed high toxicity against HepG2 cells for higher concentrations (>250 µg/mL) of Mn-Zn-Fe_2O_4/Se but were found to be non-toxic at lower concentrations. Reverse transcription polymerase chain reaction (RT-PCR) was used to evaluate gene expression of caspase 3, Bcl-2 and p53. The results were showed that the expression levelof P53 and Casp3 was clearly up-regulated, while the expression level of Bcl-2 was down-regulated (P<0.05) after hyperthermia in treated groups.

Keywords*: Mn-Zn-Fe_2O_4/Se nanocomposite; cytotoxicity;RT-PCR.*

Date of Submission: 25-08-2021 Date of Acceptance: 09-09-2021

I. Introduction

Liver cancer is the fourth major cause of cancer-related death worldwide, and according to the estimations of the World Health Organization, more than one million people will be fatal from this disease in 2030.Liver cancer represents a global health challenge, and its incidence is increasing worldwide **(Villanueva, 2019)**. It is supposed that, by 2025, more than 1 million individuals will be influenced by liver cancer every year**(Llovet*et al.*, 2021)**. Major risk factors for liver cancer involve hepatitis viral infection, additives of food, alcohol, aflatoxins, environmental and industrial toxic chemicals, water and air pollutants **(Jemal *et al.*,2007)**. Liver cancer is also emerging due to inflammation that increase deoxyribonucleic acid (DNA) damage and chromosomal abnormalities **(Buitrago-Molina *et al.*, 2013)**, It is known that both genomic instability and genetic alteration are a popular features of human liver cancer. Surgical resection has been known as the most effective method for the treatment of liver cancer**(Parks and Garden, 2001)**, but it is only showed for a small number of liver cancer patients. Radiotherapy and chemotherapy have been widely used in tumor regions but leading to fatal effects on healthy tissues **(Hildebrandt et al., 2002)**. Although these wayscan increase the intracellular temperature up to cancer cell death, they will also inflict damage at healthy tissues **(Ferrari, 2005)**. So, it is necessary to search for a new method to treat liver cancer.Magnetic fluid hyperthermia (MFH) opens a new trend for cancer treatments. Latterly, utilizing of magnetic nanoparticles (MNPs) in medical applications (e.g., magnetic fluid hyperthermia (MFH), magnetic resonance imaging and magnetic gene transfection) have had an upward trend. Hyperthermia with MNPs is a hopeful modality in the treatment of cancer. The basis of this technique is to damage cancer cells by heating them up without fatal effects on normal tissues **(Doaga*et al.*, 2013)**. In comparison with other treatment techniques, this technique is a physical therapy with little side effects, and it can be accompanied by other therapies like chemotherapy and radiotherapy to realize resistant malignant cells to these therapies **(Sun *et al.*, 2013)** and **(Heidari*et al.*, 2016)**.

MFH was firstly suggested in 1957 by **(Gilchrist *et al.*, 1957)** to damage cancer in lymph nodes by inoculated them with 'particulate matter' of maghemite and applying an alternating magnetic field (AMF) to stimulate 'selective inductive heating'.

Magnetic nanoferrites are materials that have size, magnetic properties and heating ability enough for their potential use in biomedical applications as contrast agents for magnetic resonance imaging and hyperthermia treatment **(Liu and Fan, 2014)** as Manganese zinc ferrites (Mn-Zn-Fe_2O_4), a new type of a soft magnetic material, have been widely used in biomedicine applications including magnetic resonance, imaging contrast perfection and hyperthermia, and so on. Here, they are chosen for MFH according to their high sensitivity of magnetization to temperature and low Curie temperature (Tc). The Mn-Zn-Fe_2O_4 NPs had strong absorption capabilities in the high frequency alternating magnetic field, rising to a stable temperature and showing a powerful magnetic responsiveness. Mn-Zn-Fe_2O_4 NPs have several effects on the tumor site, such as inhibition of angiogenesis (**Xie*et al.*, 2014**). Mn-Zn-Fe_2O_4 NPs also appear good biocompatibility, which proved Mn-Zn-Fe_2O_4 NPs could be used in biomedicine.

Various genomic trends have been used to explain the cancer preventing effects of selenium. It is clear from studies that selenium can void tumor progression by reversing the expression of genes involved in carcinogenesis **(El-Bayoumy K and Sinha, 2005)**. Various genes have been recognized including upregulation of genes related to phase II detoxifying enzymes **(Xiao H and Parkin, 2006**), tumor suppressor genes, selected apoptotic genes including certain caspases. In addition, selenium has been shown to change the expression of genes connected to cell cycle regulation in a modality that is consistent with growth inhibition **(Zhang et al., 2005)**.

The purpose of the present study is to evaluate the therapeutic effect of combination of MFH (thermal therapy) with chemotherapy as Mn-Zn-Fe_2O_4/Se nanocomposite on liver cancer *invivo* which are expected to be helpful for determination and controlling the temperature in hyperthermia treatments of cancer.

II. Materials And Methods

2.1) Synthesis of Mn-Zn-Fe_2O_4/Se

2.1.1) Synthesis of Mn-Zn-Fe_2O_4 nanoparticles

The thermo-sensitive Mn-Zn-Fe_2O_4 NPs were synthesized by a precipitation method. Aqueous solution of($(CH_3COO)_2Mn.4H_2O$, 98%), $(CH_3COO)_2Zn.2H_2O$, 98%), and $FeCl_3.6H_2O$, 99%, Sigma- Aldrich, St. Louis, MO, USA) were prepared. The molar concentration of these solutions was prepared as 0.05 M, 0.05 M, 0.1 M respectively in different beakers. Then, solution of $(CH_3COO)_2Zn.2H_2O$ was mixed into solution of $(CH_3COO)_2Mn.4H_2O$ at room temperature and the resulting solution was mixed into $FeCl_3.6H_2O$. The solution of NaOH (1M) (Sigma- Aldrich, St. Louis, MO, USA) at 80°C was added to the resulting solution with continuous stirring for 2 hoursat PH 12. The precipitation and formation of nanoferrites occur by conversion of metal salts into hydroxides, which occurs immediately followed by transformation of hydroxides into ferrites. After completion of reaction, the solution was filtered and was washed many times with distilled water and ethanol (70%). The particles were dried at 50°C for 3- 4 hours.

2.1.2) Synthesis of Mn-Zn-Fe_2O_4/Se nanocomposite

The resulted Mn-Zn-Fe_2O_4 NPs and atoms of Se were placed into a planetary mill for 20 minutes. A mass proportion of 90% Mn-Zn-Fe_2O_4 and 10% Se was used. Finally, the resulted composite was washed with distilled water and allowed to dry at room temperature.

2.2) Materials characterization

The phase composition and the crystallinity of the powder was detected by X-ray diffractometer using the Bruker D8 X-ray diffractometer with monochromatized Cu Ka radiation. The morphology of the obtained nanoparticles was examined with high resolution transmission electron microscope (HRTEM), (JEOL, JEM- A 2100 – Japan). To investigate the functional groups in the prepared samples the Fourier transform infra-red (FTIR) spectra of Mn-ZnFe_2O_4/Se were recorded in the range of 4000-400 cm^{-1}(Jasco Model 4100-Japan).

2.3) Cell Viability Assay

2.3.1) Cell Culture

HepG2 cell line (Research and Development Sector, The Holding Company for production of Vaccines, Sera and Drugs (VACSERA), Cairo, Egypt) was employed and cultured in Dulbecco's Modified Eagle Medium (DMEM, Sigma-Aldrich, St. Louis, MO, USA), completed with 10% fetal bovine serum (PAA Laboratories GmbH, Pasching, Austria) and (100 U/mL) Penicillin and (100 U/mL) Streptomycin (Sigma-Aldrich, St. Louis, MO, USA). The cells were incubated at 37°C temperature in 5% CO_2 atmosphere. The growth average was changed after each 24 hrs of incubation period.

2.3.2) MTT Assay

Before hyperthermia study, the cytotoxic effect of the synthesized nanocomposite was evaluated as described previously by **(Swamy et al., 2015)**. HepG2 cells were cultured at a density of 5×10^3 cells/well in a 96-well plate with 100 µL of DMEM for 48-72 hrs. Different concentrations of Mn-$ZnFe_2O_4$/Se nanocomposite (0, 15, 30, 60, 120 and 250 µg/mL) were then added to the culture medium. 3-(4,5-dimethylthiazol-2-yl) 2,5-diphenyltetrazolium bromide (MTT, 5 mg/mL) (Sigma-Aldrich, St. Louis, MO, USA). The control was set as loss of nanocomposite. The cells were incubated at 37^{o}C for 24 hrs. 10 µL of MTT reagent was supplemented to each well followed by 2–4 hrs incubation at 37^{o}C temperature. Finally, after incubation, the media were substituted by 200 µL of dimethyl sulfoxide and well mixed. Using a multi-well ELISA plate reader (Bio-tech Instruments, Winooski, VT, USA), absorbance was detected at 570 nm. The absorbance was converted to percentage of cell viability by using the subsequent equation:

RGR %(Relative growth rate) = OD of experimental group/OD of control group × 100%.

2.4) The *in vivo* therapeutical effect of Mn-$ZnFe_2O_4$/Se + MFH on cancer of the liver

2.4.1) Animal Experiment

Healthy mice (male, 10 weeks of age, 25-30 g) were obtained from the animal house of the Egyptian Organization for Biological Products and Vaccines (VACSERA), Helwan, Cairo, Egypt.All the mice were stayed atthe animal house of the Faculty of Science, South Valley University, Qena, Egypt. Mice were raised in suitable conditions with a 12 h light / dark cycle, temperature 23-25 ^{o}C, relative air humidity 20 ±5% and they were fed on pellets and water available.

2.4.2) Tumor transplantation

HepG2 cells, 5×10^{12} (Research and Development Sector, The Holding Company for production of Vaccines, Sera and Drugs (VACSERA), Cairo, Egypt) were implanted intramuscularly into the femur under ketamine (100 mg kg^{-1}, i.p.) and xylazine (10 mg kg^{-1}, i.p.) for anesthesia. When the tumor size reached about 0.7- 1cm in diameter. 40 male mice weredivided into four groups, 10 for each group. **Group I**: mice were injected intramuscularly into the femur with only HepG 2 cells (the control group (xanograft model)). **Group II:** received HepG 2 cells+Mn-Zn-Fe_2O_4*/Se* (10 mg/ml) injections only. G**roup III:** received HepG 2 cells+Mn-Zn-Fe_2O_4*/Se* (10 mg/ml) +AMF (200 kHz, 4 kW) for 30 mins performed once in each week for 2 weeks. **Group IV**: received HepG 2 cells+ Mn-Zn-Fe_2O_4*/Se* (10 mg/ml) +AMF(200 kHz, 4 kW) for 30 mins performed twice in each week for 2 weeks. The temperature was recorded with Infrared (IR) thermal camera.

2.4.3) Apoptosis-related Genes

Total RNA was extracted from control and treated tumors tissue using the Gene JET RNA Purification kit (Fermantus-UK) consistent withthe manufacturer's protocol. The concentration and the integrity of RNA were evaluated spectrophotometrically at 260/280 nm ratio. First-strand cDNA was synthesized with 1 µg of total RNA utilizing a Quantitect Reverse Transcription kit (Qiagen, Germany) in accordance with the manufacturer's instructions. These samples were subsequently frozen at a temperature of -80°C until use for determination of the expression levels of P^{53}, Casp3 and Bcl-2 genes using real-time PCR. Quantitative real-time PCR was done by a Rotor-Gene Q cycler (Qiagen, Germany) using QuantiTect SYBR Green PCR kits (Qiagen, Germany) and forward and reverse primers for each gene. Logarithmic transformation was applied on fold change values before being statistically analyzed, using the fold change values of three replicates for every gene measured. The primers sequences were as follows:

Table (A): Primers of genes

Gene	Primers
P53	F: 5'-CCC CTC CTG GCC CCT GTC ATC TTC-3' and R: 5'- GCA GCG CCT CAC AAC CTC CGT CAT-3'
Casp3	F: 5'-TTC ATT ATT CAG GCC TGC CGA GG-3' and R: 5'-TTC TGA CAG GCC ATG TCA TCC TCA-3'
Bcl-2	F: 5'-CCT GTG GAT GAC TGA GTA CC-3'and R: 5'-GAG ACA GCC AGG AGA AAT CA-3'
***β*-actin**	F: 5'-CAA GGT CAT CCA TGA CAA CTT TG-3' and R: 5'-GTC CAC CAC CCT GTT GCT GTA G-3'

2.5) Statistical analyses

Results was expressed as Means ± Standard Deviation of means (Mean ± S.D). The data were statistically analyzed by one-way ANOVAanalysis of variance (prism computer program) and the least significant difference (L.S.D) was used to test the difference between treatments. Results were represented statistically significant when P < (0.05).

III. Results

3.1) Physical results

3.1.1) X-Ray diffraction studies

The XRD of Mn-$ZnFe_2O_4$/Se nanocomposite was as shown in Fig. 1. The peaks at 2θ values of 25.82°, 35.68°, 38.27°, 57.96°,58.05°, 62.07°, 71.66° and 79.16° agreed to the crystal planes of (220), (311), (222), (422), (511) (440), (620) and (622), which confirm the formation of spinel structure of Se doped Mn–Zn ferrites(JCPDS card no. 74-2401).

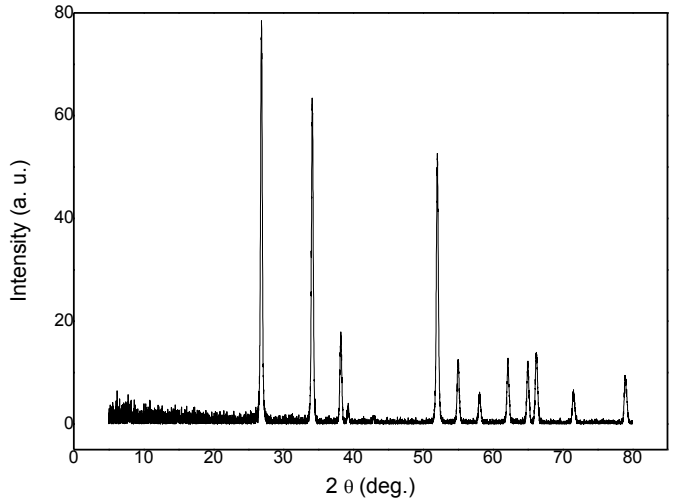

Fig 1. XRD spectra of Mn-$ZnFe_2O_4$/Se nanocomposite

The average crystallite size was determined using Scherrer equation:

$$(D = (\frac{(0.9\lambda)}{\beta\cos(\theta)})$$

where D is the average crystallite size of, λ is the incident wavelength, θ is the Brags angle and β is the diffracted full width at half maxima. The crystallite size was found to be 34.5nm.

3.1.2) Morphology Studies

The HR-TEM image of Mn-$ZnFe_2O_4$/Se sample was shown in Fig. 2.The image consists of particle- like nano - crystals. The nano-sized features are noticeably visible in the HR-TEM image.

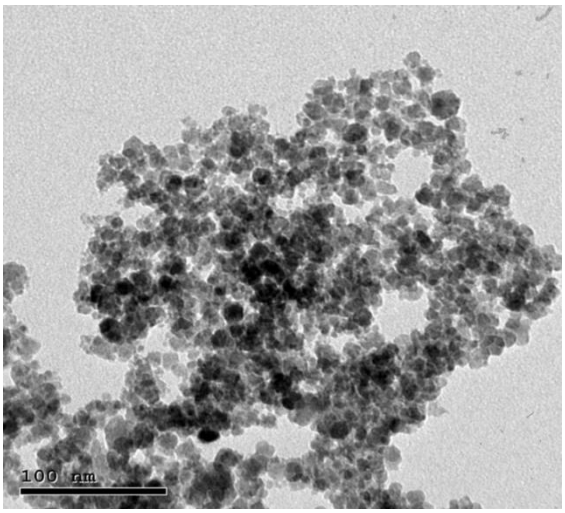

Fig 2. HRTEM of Mn-$ZnFe_2O_4$/Se nanocomposite

3.1.3) Fourier transforms infra-red spectrometer

FT-IR spectra of Mn-$ZnFe_2O_4$/Se were recorded in the range of 4000-400 cm^{-1} as shown in Fig. 3. The absorption bandseemed at 390 $cm^{-1}$and 605 $cm^{-1}$is in good agreement withvibration of Fe-O as characteristic band of spinel ferrite. The chemical bonds of the preparation particles were recognized within the spectra matching to the essential vibrations and related rotational-vibrational levels from the peaks occurred at 3401 cm^{-1}, 1624 cm^{-1}, 889 cm^{-1} and 605 cm^{-1}. The peak at 3401 cm^{-1} is due to stretching vibrations of hydroxyl group (-OH) and the peak at1624 cm^{-1} is due to -OH bonding of water. The peaks arising at 605 cm^{-1} and 889 cm^{-1}resemble to the M-O vibrational modes get up from Fe-O, Mn-O and Zn-O stretching vibrations of Mn-$ZnFe_2O_4$/Se.

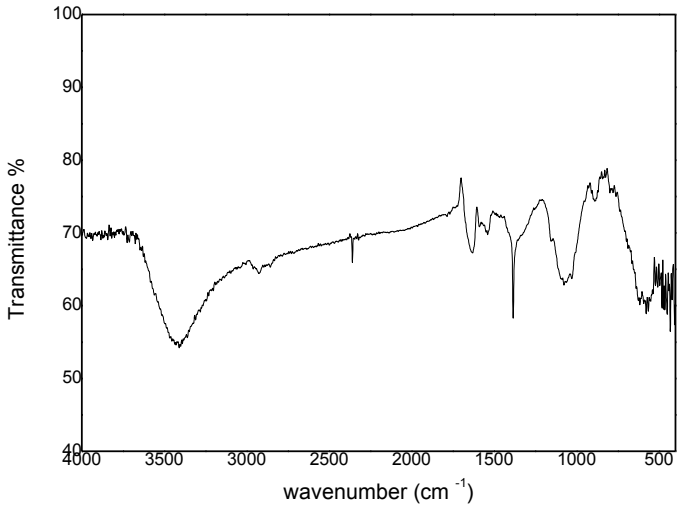

Fig 3. FTIR spectra of Mn-$ZnFe_2O_4$/Se nanocomposite

3.2) Cytotoxicity of Mn-Zn-Fe_2O_4/Se nanocomposite

The cytotoxicity activity of Mn-Zn-Fe_2O_4/Se nanocomposite at several concentrations against HepG2 (human heptacarcinoma cell line) using MTT assay is recorded in table (1) and illustrated in (Fig. 4).The results indicated that the dose dependent cytotoxicity effect of Mn-Zn-Fe_2O_4/Se nanocomposite. The highest cell viability (100%) observed at0 µg/mL (control group) began to reduce gradually with the increased concentrations. The highest toxicity effect was observed at 500 µg/mL where 42.5% cell viability was observed after 24 hrs. Interestingly, Mn-Zn-Fe_2O_4/Se nanocomposite were observed to be less toxic at lower concentrations reach to 125 µg/mL where about 72.30% of the cells were viable. However, concentrations above 250 µg/mL exhibited higher toxicity towards HepG2 cells.

Table (1) The results of cytotoxicity of Mn-Zn-Fe_2O_4/Se nanocomposite evaluated by MTT assay (± s, n = 5).

Groups	Optical Denisty (OD)	RGR %
Control group	0.055±0.002	100
15 µ/ml	0.075±0.002	91.12
30 µ/ml	0.071±0.001	85.79
60 µ/ml	0.069±0.006	82.84
125 µ/ml	0.060±0.0006	72.30
250 µ/ml	0.047±0.001	48.52

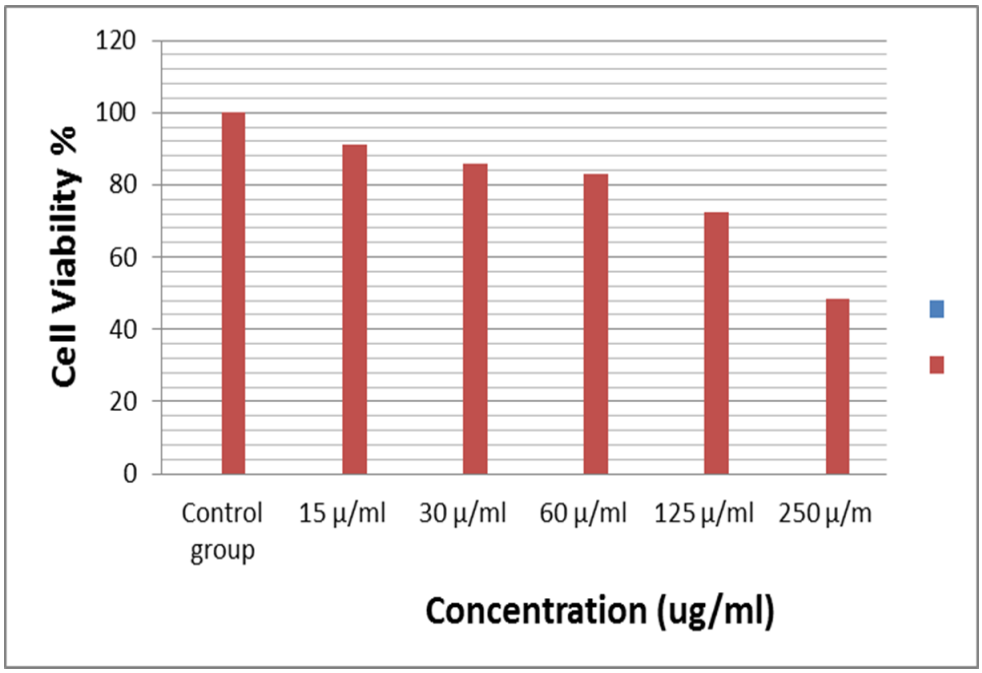

Figure (**4**): The cytotoxic effect of synthesized Mn-Zn-Fe_2O_4/Se nanocomposite on HepG2 cells (human heptacarcinoma cell line). Each value is expressed as a mean of ± S.D (*n* = 5).

3.3) Apoptosis-related Genes

3.3.1) Effect of AMF induced Mn-Zn-Fe_2O_4/Se nanocomposite-mediated hyperthermia treatment on RT-PCR

mRNA expression levels of apoptosis-related Genes, data in table (1) showed that the level of expression of proapoptotic genes (P53 and Casp3) was clearly up-regulated, while the expression level of anti-apoptotic genes (Bcl-2) was down-regulated ($P<0.05$) after hyperthermia in MFH 1 and MFH 2 groups, indicating its potential effectiveness in directing cancer cells toward programmed death (Fig.5).

Table (2)Effect of AMF induced Mn-Zn-Fe_2O_4/Se nanocomposite-mediated hyperthermia treatment on RT-PCR

Groups Gene expression	P53	Bcl-2	Casp-3
Control group	**1**	**1**	**1**
MF group	**3.508±0.0114**	**0.755±0.0100**	**2.274±0.0364**
MFH 1	**4.359±0129**	**0.634±0.0060**	**3.677±0.0926**
MFH 2	**4.983±0.0300**	**0.432±0.0062**	**5.331±0.0329**

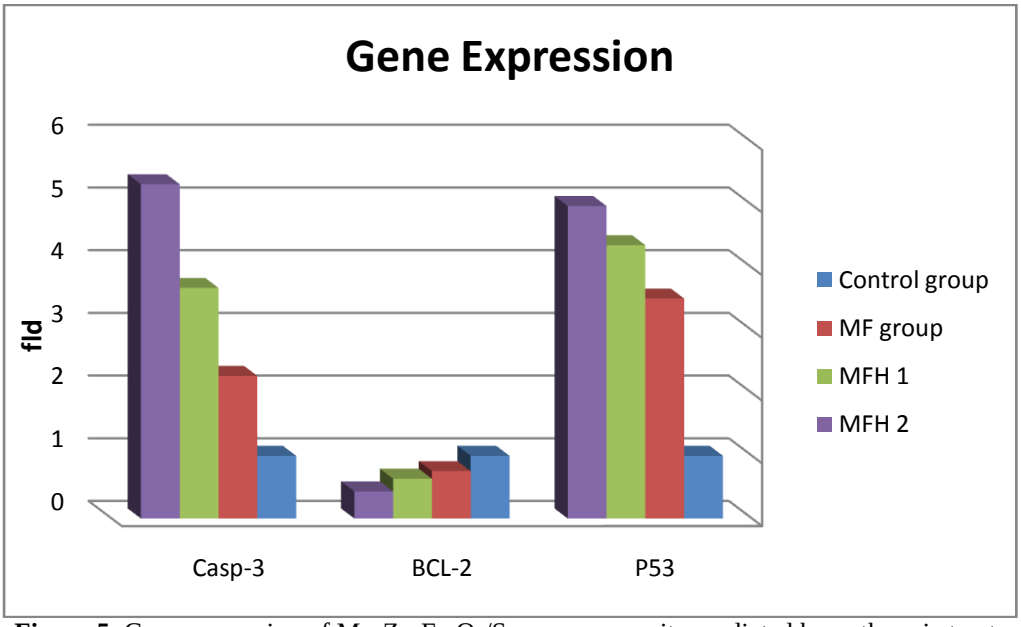

Figure 5: Gene expression of Mn-Zn-Fe_2O_4/Se nanocomposite-mediated hyperthermia treatment on RT-PCR, Control group: saline solution.MF group: Mn-Zn-Fe_2O_4/Se only MFH 1 group: Mn-Zn-Fe_2O_4/Se+AMF once per week for 2 weeks MFH 2 group: Mn-Zn-Fe_2O_4/Se+AMF twice per week for 2 weeks

Figure (5) shows the expression of P53, BCL-2 and Caspase-3 in all experimental groups (control, MF, MFH 1 and MFH 2 groups). As appears in this figure P53 and Caspase-3 increased in the treated groups but, BCL-2 decreased in the treated groups.

IV. Discussion

Hyperthermia (HT) is a therapeutic tumor treatment which rises the temperature at the tumor site. The temperature increasing alterations the physiology of the tumor cells resulting in selective death through apoptosis **(Moy and Tunnell, 2017)**, accordingly to the temperature values reached during the treatment. HT might be classified in three categories: diathermia, where the temperature is less than 41°C, typically employed for rheumatic diseases; moderate hyperthermia, which causes stress to the cells within the temperature range of 41–46 °C; and thermoablation, where the temperature rises to 56 °C, causing cells necrosis **(Mallory et al., 2016)**.After the HT treatment, several alterations occur in the cell, such as the reduction in the transmembrane transport, the destabilisation of the membrane potential and the changes in the structural proteins **(Moy and Tunnell, 2017)**. Furthermore, also the synthesis of the nucleic acid and the DNA repairing enzymes are affected by increasing the temperature, altering the conformation of the DNA and leading to cell death **(Silva et al., 2011)**. In Magnetic Hyperthermia Therapy (MHT), the heating of the target tissue is obtained by injecting magnetic nanoparticles (MNPs) *in* tumor and then exposing the body part to an alternating current (AC) magnetic field **(Mertz et al., 2017)**. Magnetic energy is converted to heat by MNPs and transferred to the tumor tissue**(Deatsch and Evans, 2014)**.

In this study, we shed some light on synthesis of Mn-Zn-Fe2O4/Se nanocomposite, evaluate the therapeutic of Mn-Zn-Fe_2O_4 when combine with Se that represent as chemotherapy and perform in vivo studyusing this nanocomposite under an alternating magnetic field on liver cancer treatment.

XRD and FTIR results prove the preparation of nanocrystalline Mn-Zn-Fe2O4/Se nanocomposite. TEM results indicated the synthesized of Mn-Zn-Fe2O4/Se nanocomposite was shown to be uniformly distributed and almost spherical in shape and possess high biocompatibility that are important for biomedical applications. These results agree with **Kanagesan*et al.* (2016)**.

The results of cytotoxicity activity of Mn-Zn-Fe_2O_4/Se nanocomposite against HepG2 using MTT assay is indicated the dose dependent cytotoxicity effect of Mn-Zn-Fe_2O_4/Se nanocomposite. Similarly, previous studies also have shown the dose dependent cytotoxicity of various kinds of nanoparticles **(Akhtar *et al.*, 2015)**

Our study agrees with **Kanagesan*et al.* (2016)** illustrated that the dose dependent cytotoxicity activity of $ZnFe_2O_4$ and $CuFe_2O_4$ against MCF-7 cells with higher toxicity observed at higher concentrations of nanoparticles. Concentrations below 125µg/mL were found to be less toxic proposing their biocompatibility at lower concentrations.

Our study is in agreement with earlier reports where $CaFe_2O_4$ nanoparticles were showed to exhibit high toxicity when used above 250 ug/mL **(Khanna *et al.,* 2013)**. $ZnFe_2O_4$, $NiFe_2O_4$ nanoparticles at 100 µg/mL concentration have indicated less cell viability **(Leung *et al.,* 2010)**.

Selenium (Se) is a mineral trace element, which is very important to humans and animals and has a very important role in cancer cell, it represents a chemotherapeutic and chemopreventiveagent has been demonstrated in many epidemiological, preclinical, and clinical studies **(Giannitrapani*et al.,* 2014)**. Several studies showed that Se has antioxidant activities in vitro and in vivo through the activation of selenoenzymes such as glutathione peroxidase (GPx) and thioredoxin reductase (TrxR) which stop oxidative damage to body tissues **(Horky*et al.,* 2016)**.

Accumulating evidences show that chemotherapeutic agents stimulate tumor degradation through inhibition of proliferation and/or activation of apoptosis. Apoptosis has been recognized as a critical mechanism for cancer chemoprevention by Se compounds and changes that occurred during apoptosis, involving cell shrinkage, formation of apoptotic bodies, accumulation of sub-G1 cell population and nuclear condensation were observed in cancer cells treated with various concentrations of Se **(Chung*et al.,* 2011)**.

Apoptosis is a genetically structured cellular death process activated by different internal and external signals. The effective mitochondrial apoptosis pathway is triggered by intracellular stimuli that upregulate the pro-apoptotic BCL-2 family of proteins, such as Bax, Bad (Bcl-2 associated aganist of cell death), and Bak (Bcl-2 homologous antagonist/killer), leading to the mitochondrial release of cytochrome C **(Linehan *et al.,* 2003)** and **(You *et al.,* 2017)**. This intracellular stress (stimuli) should be strong enough to be able to run the apoptosis pathway in the cells; otherwise, some anti-apoptosis molecules would be activated and decrease the cellular apoptosis procedure. In our study, the magnetic hyperthermia treatment was able to trigger the effective apoptosis pathway and overcome the heat shock proteins (HSP) that cause thermal resistance in cancer cells **(Ikwegbue*et al.,* 2017)**.

In the current study mRNA expression of P53 and caspase-3 through RT-PCR technique was significantly increase but, Bcl-2 was significantly decrease in treated group than that of control and magnetic nanoparticles only group, these results were in agree with a study in **(Thorgeirsson*et al.,* 1998)**, they explained the mechanism through the decreases of the expression of antiapoptotic members of the BCL-2 family and increases the expression of p53, Bax, and procaspases 3, 8, and 9.

Our study agree with **Salimi*et al*. (2020)** when employing dendrimer functionalized iron oxide nanoparticles in treatment of breast Cancer-bearing BALB/c Mice with magnetic hyperthermia and indicated that the expression of Bax in cancer cells increased significantly after magnetic hyperthermia treatment (MNPs + AMF) compared to that in control group; Furthermore, Bcl-2 expression decreased significantly in the group of MNPs+AMF.

Authors haveconfirm that the improved apoptotic effect of hyperthermia occurs byalternating the expression of apoptosis genes, like p53, Bcl-2 and Bax**(Liang *et al.,* 2007)**. Other authors have experimentally appeared, at least in melanoma, that the apoptotic effect of HT is gained by activating not caspases 8 or 9 but activating a nonconventional apoptotic pathway caspases 3, 7 **(Shellman*et al.,* 2008)**.

V. Conclusion

Hepatocellular carcinoma (HCC) is one of most popular malignant tumors in worldwide and the incidence of HCC reported has obviously increased in recent years. Despite a variety of therapeutic strategies, HCC remains a significant reason of cancer death. Therefore, to search for a new method to treat HCC is of the most importance. So, using MFH with chemotherapy is a promising method in the treatment of cancer due to their biocompatibility, stability, and unique structurefor the coupling of biomolecules. The Mn-Zn-Fe_2O_4/Se nanocomposites presented in this study was suitable for magnetic hyperthermia treatment of liver cancer. The real time-PCR results also showed that magnetic hyperthermia with chemotherapy treatment was capable of regulating the expression of the apoptosis-related genes. This study maypromote a new method of target therapy for liver cancer and other solid tumors. To the best of our knowledge, this is the first study of its form, that shows the utility of Mn-Zn-Fe_2O_4/Se nanocomposites- mediated hyperthermia for cancer treatment in an animal model.

ACKNOWLEDGMENTS

The authors are grateful to Dr. Alaa H. Said for excellent technical assistance and for supporting the purchase of some reagents.

CONFLICT OF INTEREST

The authors declare no conflict of interest in this work.

References

Akhtar, M., Swamy, M. K., Umar, A. and Al Sahli, A. A. (2015). Biosynthesis and characterization of silver nanoparticles from methanol leaf extract of Cassia didymobotyra and assessment of their antioxidant and antibacterial activities. *Journal of nanoscience and nanotechnology*, *15*, 9818-9823.

Buitrago-Molina, L. E., Marhenke, S., Longerich, T., Sharma, A. D., Boukouris, A. E., Geffers, R., Manns, M. P. and Vogel, A. (2013). The degree of liver injury determines the role of p21 in liver regeneration and hepatocarcinogenesis in mice. *Hepatology*, *58*, 1143-1152.

Carcinoma Villanueva, A. (2019). Hepatocellular. *N Engl J Med*, *380*, 1450-1462.

Chung, C. Y., Madhunapantula, S. V., Desai, D., Amin, S. and Robertson, G. P. (2011). Melanoma prevention using topical PBISe. *Cancer Prevention Research*, *4*, 935-948.

Deatsch, A. E. and Evans, B. A. (2014). Heating efficiency in magnetic nanoparticlehyperthermia. *Journal of Magnetism and Magnetic Materials*, 354, 163-172.

Doaga, A., Cojocariu, A. M., Amin, W., Heib, F., Bender, P., Hempelmann, R. and Caltun, O. F. (2013). Synthesis and characterizations of manganese ferrites for hyperthermia applications. *Materials Chemistry and Physics*, *143*, 305-310.

El-Bayoumy, K. and Sinha, R. (2005). Molecular chemoprevention by selenium: a genomic approach. *Mutation Research/Fundamental and Molecular Mechanisms of Mutagenesis*, *591*, 224-236.

Ferrari, M. (2005). Cancer nanotechnology: opportunities and challenges. *Nature reviews cancer*, *5*, 161-171.

Giannitrapani, L., Soresi, M., Bondì, M. L., Montalto, G. and Cervello, M. (2014). Nanotechnology applications for the therapy of liver fibrosis. *World Journal of Gastroenterology: WJG*, *20*, 7242.

Gilchrist, R. K., Medal, R., Shorey, W. D., Hanselman, R. C., Parrott, J. C. and Taylor, C. B. (1957). Selective inductive heating of lymph nodes. *Annals of surgery*, *146*, 596.

Heidari, M., Sattarahmady, N., Javadpour, S., Azarpira, N., Heli, H., Mehdizadeh, A., Rajaei, A. and Zare, T. (2016). Effect of magnetic fluid hyperthermia on implanted melanoma in mouse models. *Iranian journal of medical sciences*, *4Z*, 314.

Hildebrandt, B., Wust, P., Ahlers, O., Dieing, A., Sreenivasa, G., Kerner, T., Felix, R. and Riess, H. (2002). The cellular and molecular basis of hyperthermia. *Critical reviews in oncology/hematology*, *43*, 33-56.

Horky, P., Ruttkay-Nedecky, B., Nejdl, L., Richtera, L., Cernei, N., Pohanka, M., Kopel, P., Skladanka, J., Hloucalova, P., Slama, P., Nevrkla, P., Mlejnkova, V., Klusonova, V., Kizek, R. and Adam, V. (2016). Electrochemical methods for study of influence of selenium nanoparticles on antioxidant status of rats. *International Journal of Electrochemical Science*, *11*, 2799-2824.

Ikwegbue, P. C., Masamba, P., Oyinloye, B. E. and Kappo, A. P. (2018). Roles of heat shock proteins in apoptosis, oxidative stress, human inflammatory diseases, and cancer. *Pharmaceuticals*, *11*, 2.Magnetic

Jemal, A., Siegel, R., Ward, E., Murray, T., Xu, J. and Thun, M. J. (2007). Cancer statistics, 2007. *CA: a cancer journal for clinicians*, *57*, 43-66.

Kanagesan, S., Hashim, M., AB Aziz, S., Ismail, I., Tamilselvan, S., Alitheen, N. B., Swamy, M. K. and Purna Chandra Rao, B. (2016). Evaluation of antioxidant and cytotoxicity activities of copper ferrite (CuFe2O4) and zinc ferrite (ZnFe2O4) nanoparticles synthesized by sol-gel self-combustion method. *Applied Sciences*, *6*, 184.

Khanna, L. and Verma, N. K. (2013). Synthesis, characterization and in vitro cytotoxicity study of calcium ferrite nanoparticles. *Materials science in semiconductor processing*, *16*, 1842-1848.

Leung, K. C. F. and Wang, Y. X. J. (2010). Mn–Fe nanowires towards cell labeling and magnetic resonance imaging. *Nanowires science and technology*, 331-344.

Liang, H., Zhan, H. J., Wang, B. G., Pan, Y. and Hao, X. S. (2007). Change in expression of apoptosis genes after hyperthermia, chemotherapy and radiotherapy in human colon cancer transplanted into nude mice. *World Journal of Gastroenterology: WJG*, *13*, 4365.

Linehan, W. M., Walther, M. M. and Zbar, B. (2003). The genetic basis of cancer of the kidney. *The Journal of urology*, *170*, 2163-2172.

Liu, X. L. and Fan, H. M. (2014). Innovative magnetic nanoparticle platform for magnetic resonance imaging and magnetic fluid hyperthermia applications. *Current Opinion in Chemical Engineering*, *4*, 38-46.

Llovet J. M., Kelley, R. K., Villanueva, A., Singal, A. G., Pikarsky, E., Roayaie, S., Lencioni, R., Koike, K., Zucman- Rossi, J. and Finn, R. S. (2021). Hepatocellular Carcinoma. *NATURE REVIEWS*, 7:6

Mallory, M., Gogineni, E., Jones, G. C., Greer, L., & Simone II, C. B. (2016). Therapeutic hyperthermia: The old, the new, and the upcoming. Critical reviews in oncology/hematology, 97, 56-64.

Mertz, D., Sandre, O. and Begin-Colin, S. (2017). Drug releasing nanoplatforms activated by alternating magnetic fields. *Biochimica et Biophysica Acta (BBA)-General Subjects*, *1861*, 1617-1641.

Moy, A. J. and Tunnell, J. W. (2017). Combinatorial immunotherapy and nanoparticle mediated hyperthermia. *Advanced drug delivery reviews*, 114, 175-183.

Parks, R. W. and Garden, O. (2001). Liver resection for cancer. *World journal of gastroenterology*, *7*, 766.

Salimi, M., Sarkar, S., Hashemi, M. and Saber, R. (2020). Treatment of breast cancer-bearing balb/c mice with magnetic hyperthermia using dendrimerfunctionalizediron-oxide nanoparticles. *Nanomaterials*, *10*,2310.

Shellman, Y. G., Howe, W. R., Miller, L. A., Goldstein, N. B., Pacheco, T. R., Mahajan, R. L., LaRue, M. S. and Norris, D. A. (2008). Hyperthermia induces endoplasmic reticulum-mediated apoptosis in melanoma and non-melanoma skin cancer cells. *Journal of investigative dermatology*, *128*, 949-956.

Silva, A. C., Oliveira, T. R., Mamani, J. B., Malheiros, S. M., Malavolta, L., Pavon, L. F., Sibov, T. T., Amaro Jr, E., Tannús, A., Vidoto, E. L. G., Martins, M. J., Santos, R. S. and Gamarra, L. F. (2011). Application of hyperthermia induced by superparamagnetic iron oxide nanoparticles in glioma treatment. *International journal of nanomedicine*, *6*, 591.

Sun, H., Xu, L., Fan, T., Zhan, H., Wang, X., Zhou, Y. And Yang, R. J. (2013). Targeted hyperthermia after selective embolization with ferromagnetic nanoparticles in a VX2 rabbit liver tumor model. *International journal of nanomedicine*, *8*, 3795.

Swamy, M. K., Sudipta, K. M., Jayanta, K. and Balasubramanya, S. (2015). The green synthesis, characterization, and evaluation of the biological activities of silver nanoparticles synthesized from Leptadenia reticulata leaf extract. *Applied nanoscience*, *5*, 73-81.

Thorgeirsson, S.S., Teramoto, T. and Factor, V. M. 1998. Dysregulation of apoptosis in hepatocellular carcinoma. *Semin Liver Disease*, *18*, 115–22.

Xiao, H. and Parkin, K. L. (2006). Induction of phase II enzyme activity by various selenium compounds. *Nutrition and cancer*, *55*, 210-223.

Xie, J., Zhang, Y., Yan, C., Song, L., Wen, S., Zang, F., Chen, G., Ding, Q., Yan, C. and Gu, N. (2014). High-performance PEGylated Mn–Zn ferrite nanocrystals as a passive-targeted agent for magnetically induced cancer theranostics. *Biomaterials*, *35*, 9126-9136.

You, Y., Cheng, A. C., Wang, M. S., Jia, R. Y., Sun, K. F., Yang, Q.,Wu, Y., Zhu, D., Chen, S., Liu, M. F,. Zhao, X. X and Chen, X. Y. (2017). The suppression of apoptosis by-herpesvirus. Cell Death Disease, *8*: 2749.

Zhang, H., Dong, Y., Zhao, H., Brooks, J. D., Hawthorn, L., Nowak, N., Marshall, J. R., Gao, A.C. and Ip, C. (2005). Microarray data mining for potential selenium targets in chemoprevention of prostate cancer. *Cancer Genomics-Proteomics*, *2*, 97-113.